Applied General Topology

Appl. Gen. Topol. 20, no. 1 (2019), 251-264
doi:10.4995/agt.2019.10928
© AGT, UPV, 2019

Exact computation for existence of a knot counterexample

K. Marinelli and T. J. Peters

Department of Computer Science & Engineering, University of Connecticut, USA
(kevin.marinelli@uconn.edu,tpeters@cse.uconn.edu)

Communicated by M. Schellekens

Abstract

Previously, numerical evidence was presented of a self-intersecting Bézier curve having the unknot for its control polygon. This numerical demonstration resolved open questions in scientific visualization, but did not provide a formal proof of self-intersection. An example with a formal existence proof is given, even while the exact self-intersection point remains undetermined.

2010 MSC: *68U05.*

Keywords: *knot theory; isotopy; parametric curve.*

1. Introduction to Existence Condition for Self-intersection

The formal proof of an unknotted control polygon with a self-intersecting Bézier curve (See Definition 3.3.) appears in Theorem 8.4. The progression in Figure 1, from left to right, shows 'snap shots' of a piecewise linear (PL) curve being linearly perturbed, generating new Bézier curves at each instant. The top-most point is the only one perturbed. The initial (left) and final (right) Bézier curves are shown to have differing prime knot types, so there must be an intermediate Bézier curve with a self-intersection (as shown in the middle image by a black dot). Relevant definitions follow.

Received 25 April 2018 – Accepted 06 November 2018

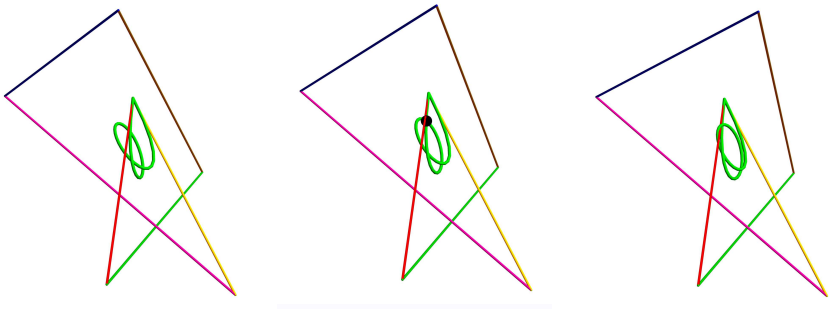

FIGURE 1. Existence of self-intersection

2. Data for the Example

Let

$$(0, 9, 20), (-15, -95, -50), (40, 80, -20), (\mathbf{-10}, \mathbf{-60}, \mathbf{58}),$$
$$(-60, 30, 20), (40, -60, -60), (0, 9, 20)$$

be the ordered list of vertices for the initial PL knot, denoted by K_0. Integer values are chosen for exact computation. In Figure 1, the vertex $(0, 9, 20)$ is the initial and final point of the Bézier curves (shown as the highest point on the polynomial curve, colored green). The remaining vertices are arranged counterclockwise. A single Reidemeister move of vertex (40, -60, -60) shows that K_0 is the unknot.

The vertex in bold font is perturbed linearly to $(\mathbf{10}, \mathbf{-60}, \mathbf{58})$ to obtain the final PL knot, denoted by K_1, with all other vertices remaining fixed. The perturbation generates uncountably many new control polygons and associated Bézier curves. The Bézier curves corresponding to K_0 and K_1 are denoted by β_0 and β_1, respectively. Both K_0 and K_1 resulted from visual experiments.

3. Mathematical Preliminaries

Some relevant mathematical definitions are summarized.

Definition 3.1. A subspace of $\mathbf{R}^3$ is called a knot [7] if it is homeomorphic to a circle.

The stronger equivalence of ambient isotopy is fundamental in knot theory.

Definition 3.2. Let X and Y be two subspaces of $\mathbb{R}^3$. A continuous function

$$H : \mathbb{R}^3 \times [0, 1] \to \mathbb{R}^3$$

is an **ambient isotopy** between X and Y if H satisfies the following conditions:

(1) $H(\cdot, 0)$ is the identity,
(2) $H(X, 1) = Y$, and
(3) $\forall t \in [0, 1], H(\cdot, t)$ is a homeomorphism from $\mathbb{R}^3$ onto $\mathbb{R}^3$.

Definition 3.3. Denote $\mathcal{C}(t)$ as the parameterized Bézier curve of degree n with control points $P_i \in \mathbf{R}^3$, defined by

$$\mathcal{C}(t) = \sum_{i=0}^{n} B_{i,n}(t) P_i, \quad t \in [0,1],$$

where $B_{i,n}(t) = \binom{n}{i} t^i (1-t)^{n-i}$.

The curve $\mathcal{P}$ formed by PL interpolation on the ordered list of points

$$P_0, P_1, \ldots, P_n$$

is called the *control polygon* and is a PL approximation of $\mathcal{C}$.

The work presented was partially motivated by development of wireless data gloves. The smooth Bézier representations are manipulated by the gloves, while the illustrative computer graphics are created by PL approximations derived from the control polygon. Topological fidelity between these representations is of interest to provide reliable visual feedback to the user.

4. Related Work

This article arose from a question posed by a referee[1] from a previous numerical example [22].

The mathematical objects of study here are Bézier curves. The canonical references [13] (any edition) and [27] focus on approximation and modeling, with less attention to associated topological properties. Relations between a smooth curve and its PL approximation are dominant in computer graphics [14], but the topological aspects are often ignored. One prominent property is that any Bézier curve is contained in the convex hull of its control points [13], while recent enhancements have been shown [26], where the containing set is a subset of the convex hull.

The *push* receives prominent attention by R. H. Bing [8] as a fundamental tool in developing ambient isotopies in $\Re^2$. The perturbation in this article is the trivial extension of a push to $\Re^3$.

The preservation of topological characteristics in geometric modeling and graphics has become of contemporary interest [4, 5, 6, 10, 12, 16, 19, 21]. Sufficient conditions for a homeomorphism between a Bézier curve and its control polygon have been studied [25], while topological differences have also been shown [9, 22, 27].

Topological aspects are relevant in 'molecular movies' [23]. Sufficient conditions were established for preservation of knot type [17] during dynamic visualization of ongoing molecular simulations [29]. Interest by bio-chemists in using hand gestures to interactively manipulate these complex molecular images prompts related topological considerations for data gloves [1, 2, 3].

[1]Author T. J. Peters thanks that referee of the previous numerical work [22] for a suggestion that led to the example shown here.

The beautiful visual studies of knot symmetry [28] provided an example of the 7_4 knot that was helpful in the initial visual studies performed to create the example presented here.

Exact computation has some advantages over floating point arithmetic [11, 18], particularly regarding loss of precision in finite bit strings, with alternative views expressed [15]. Some *ad hoc* techniques are often invoked to provide adequate bit length for full precision relative to a particular computation, as has been done here.

5. Exact Computation for Subdivision

The de Casteljau algorithm [13] is a subdivision method for Bézier curves[2]. The algorithm recursively generates control polygons that more closely approximate the curve [13] under Hausdorff distance [24]. The algorithm is presented here, for a Bézier curve denoted by α, for the input value of $t = 1/2$, as is customary[3]. The point $\alpha(1/2)$, is an endpoint output by the algorithm. For $t = 1/2$ subdivision proceeds by selecting the midpoint of each edge of the control polygon and these midpoints are connected to create new edges, as shown in the left image of Figure 2. Recursive creation and connection of midpoints continues until an edge is created that is tangent to the Bézier curve [13]. Termination is guaranteed since there are only finitely many edges.

This splits the original curve into two pieces, at $\alpha(1/2)$, designated here as the 'left' and 'right' pieces of α. The left piece has a control polygon with a final point of $\alpha(1/2)$ and the right piece has a control polygon with initial point of $\alpha(1/2)$, as shown in the right image of Figure 2, where $\alpha(1/2)$, is the point of tangency for terminating the algorithm. The union of the edges from the final step then forms two new PL curves (each described as a sub-control polygon[4]) as shown in blue and green in the right image of Figure 2.

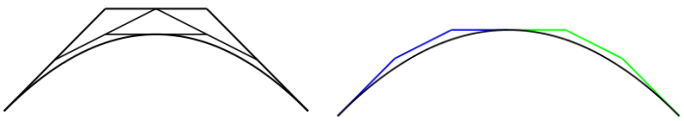

Figure 2. A subdivision of a cubic Bézier curve at parameter $\frac{1}{2}$

For each iteration, m, the subdivision process generates 2^m PL sub-curves, each being a sub-control polygon [13], as denoted by $\mathcal{P}_j^m$ for $j = 1, 2, 3, \ldots, 2^m$. For a Bézier curve initially defined by $n+1$ control points, each $\mathcal{P}_j^m$ has $n+1$ points and their union $\bigcup_j \mathcal{P}_j^m$ forms a new PL curve that converges in Hausdorff distance to the original Bézier curve. The Bézier curve defined by $\bigcup_j \mathcal{P}_j^m$ is exactly the same as the original Bézier curve [20].

[2]An illustrative image appears [13, Figure 3.2].
[3]Any parameter t from $(0, 1)$ can be substituted.
[4]Note that each sub-control polygon of a simple Bézier curve is open.

© AGT, UPV, 2019

Remark 5.1. A Bézier curve is contained within the convex hull of its control points [13].

Remark 5.1 also applies to each sub-control polygon, as will be extensively used. The stick knots of Section 2 are refined via the DeCasteljau subdivision algorithm, repeatedly computing averages for the coordinate vertices in the form $\frac{(a+b)}{2}$. In order to retain integer valued vertices throughout all computed subdivisions, the vertices will be scaled by 2^k, for an appropriately chosen k. The existence of self-intersections in the Bézier curves is preserved under scaling. Each subdivision iteration has one division by 2 for each degree d. In our examples, we invoke ℓ levels of subdivision, so that $k = \ell * (d + 1) + 1$.

6. Ambient Isotopy Between Stick Knots

The two curves, K_0 and K_1 will be shown to be the unknot.

Lemma 6.1. *The curve K_0 is the unknot.*

Proof. The demonstration that K_0 is simple proceeds directly over the six edges. The non-consecutive pairs of edges have separating hyperplanes. □

Lemma 6.2. *The curves K_0 and K_1 are ambient isotopic.*

Proof. The single perturbation to create K_1 is similar to a push [8] and incurs no self-intersections with other segments. It is easily extended to an ambient isotopy having compact support. □

Corollary 6.3. *The curve K_1 is the unknot.*

7. Subdivision Analysis

The points from the 4th iteration of the DeCasteljau algorithm, using a subdivision value of $1/2$ are listed in Appendix A. These can be verified simply by executing the algorithm on the initial data for K_0 and K_1, with the provision that the implementation relies upon exact arithmetic.

It was observed that each sub-control polygon in Appendix A had the property that its control points were strictly monotone in one of its coordinate values. This is annotated in the appendix by abbreviations noting the coordinates in which strict monotonicity was observed. In some cases, this occurs for all three coordinates. This observation greatly simplified the proofs presented.

Let $K_{0,4}$ denote the PL curve formed from the 4th subdivision on K_0 and similarly denote $K_{1,4}$ for K_1. Within each of $K_{0,4}$ and $K_{1,4}$, there are 16 sub-control polygons. The rest of the paper proceeds by showing that $K_{0,4}$ is the unknot and is ambient isotopic to β_0 and that $K_{1,4}$ is the trefoil and is ambient isotopic to β_1. As the convex hulls of the sub-control polygons become central, their images are shown in Figure 3.

Lemma 7.1. *Both $K_{0,4}$ and $K_{1,4}$ are simple.*

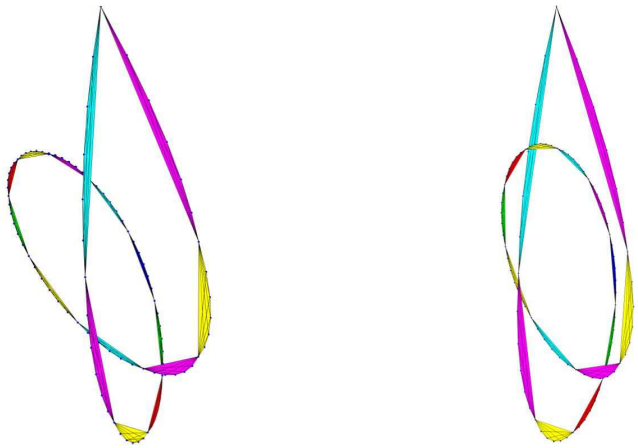

(a) K_0 (b) K_1

FIGURE 3. Convex Hulls – Fourth subdivision (parameter $\frac{1}{2}$)

Proof. First consider $K_{0,4}$. Let $K_{0,4,i}$, for $i = 0, 1, \ldots 15$, denote the 16 sub-control polygons for $K_{0,4}$. Each $K_{0,4,i}$, for $i = 0, 1, \ldots 15$, is simple, because of the strict monotonicity in at least one coordinate. The $K_{0,4,i}$, for $i = 0, 1, \ldots 15$, are pairwise disjoint (except at shared endpoints), as established by computing the convex hull for each. Again, any ambiguity that could arise from floating point arithmetic is avoided by exact computations.

The argument for $K_{1,4}$ follows the same pattern. □

The derivative of a Bézier curve $\mathcal{C}$ is expressed as

$$\mathcal{C}^{'}(t) = \sum_{i=0}^{n} \binom{n}{i} t^i (1-t)^{n-i} (P_{i+1} - P_i), i \in \{1, \ldots, n-1\}.$$

Lemma 7.2. *Each of β_0 and β_1 are strictly monotonic in the same coordinate as their corresponding control polygons and are simple.*

Proof. The strict monotonicity in some coordinate for each sub-control polygon implies that the partial derivative in the x, y or z variable will be positive, implying simplicity for that segment of the Bézier curve. Since each Bézier segment is contained in the convex hull of its sub-control polygon and since those convex hulls are pairwise disjoint (except at shared endpoints), the simplicity follows. □

Corollary 7.3. *If a control polygon is strictly monotonic in some coordinate, then its associated Bézier curve is also.*

Subdivision need not preserve knot type, so we consider $K_{0,4}$ and $K_{1,4}$.

Lemma 7.4. *The curve $K_{0,4}$ is the unknot.*

Proof. Project $K_{0,4}$ onto the $X-Y$ plane, where 3 intersections are computed exactly, listed according to the oriented direction of $K_{0,4}$, with the z coordinates also computed exactly.

Overcrossing at $(x, y) =$

$$(70600874219532518400/90998355737, -331936500725210686464/90998355737),$$
$$\text{since } z\text{: } 346821834258400839680/90998355737 > -179855360,$$

Overcrossing at $(x, y) =$

$$(-2606810091676070400/2228701007, -1412989965727044111136/15600907049),$$
$$\text{since } z\text{: } -695629074309606400/821100371 > -2734161920,$$

Undercrossing at $(x, y) =$

$$(70736463317966883840/46441845451, -21833139014382396303 36/232209227255),$$
$$\text{since } z\text{: } -312474348049921062912/46441845451 < -5234410880.$$

This crossing information permits the conclusion that $K_{0,4}$ is the unknot. □

Lemma 7.5. *The curve $K_{1,4}$ is the trefoil.*

Proof. Project $K_{1,4}$ onto the $X-Y$ plane, as done, similarly, in the proof of Lemma 7.4, with, again, 3 intersections computed exactly.

Undercrossing at $(x, y) =$

$$(-232151158892789760 0/2778711187, -1286006491729782374 4/2778711187),$$
$$\text{since } z\text{: } = 8352902508791726080/2778711187 < 4026531840,$$

Overcrossing at $(x, y) =$

$$(-821724978383994880 0/7079707793, -588354638932543733 76/7079707793),$$
$$\text{since } z\text{: } = -24693447116718080/7079707793 > -1547779858,$$

Undercrossing at $(x, y) =$

$$(27367109371614504 96/968030497, -222045650166834551808/24200762425),$$
$$\text{since } z\text{: } = -644329182006659481 6/968030497 < -5348303360.$$

These three pairs of alternating crossings permit conclusion of the trefoil. □

8. Ambient Isotopy for Bézier Curves

We show that β_0 is ambient isotopic to $K_{0,4}$ and that β_1 is ambient isotopic to $K_{1,4}$. Both proofs proceed by showing that each sub-control polygon is ambient isotopic to its associated Bézier curve. We show this for one sub-control polygon, as representative. Let $K_{0,4,i}$ be one such control polygon and let $\beta_{0,i}$ be its corresponding Bézier curve segment.

Theorem 8.1. *Each $K_{0,4,i}$ is ambient isotopic to its corresponding Bézier curve, denoted as $\beta_{0,i}$.*

Proof. Without loss of generality assume $K_{0,4,i}$ is strictly monotonic in its x coordinate, which implies that $\beta_{0,i}$ is also strictly monotonic in its x coordinate by Corollary 7.3. For each $p \in K_{0,4,i}$, let Π_p be the plane at p that is parallel to the YZ-plane. By the indicated strict monotonicity, $\Pi_p \cap K_{0,4,i} = \{p\}$, is a unique point. Similarly, by the same strict monotonicity on $\beta_{0,i}$, the intersection $\Pi_p \cap \beta_{0,i}$ has at most one point, and the connectivity of $\beta_{0,i}$ (as the continuous image of a connected subset of $[0,1]$) implies that this intersection is non-empty. For each $p \in K_{0,4,i}$, let $q_p = \Pi_p \cap \beta_{0,i}$. To construct the ambient isotopy, consider the line segment between each p and q_p. The interiors of these line segments will not intersect, due to the strict monotonicity. The remaining details to construct an ambient isotopy of compact support are standard and left to the reader. □

Corollary 8.2. *The Bézier curve β_0 is ambient isotopic to its control polygon $K_{0,4}$, the unknot.*

Proof. The existence of an ambient isotopy within each convex hull of $K_{0,4,i}$, the lack of intersection between convex hulls $K_{0,4,i}$ and $K_{0,4,j}$ for $i \neq j$ (except at the end points when $j = i + 1$, where those end points remain fixed) and composition of the ambient isotopies on each sub-control polygon conclude this proof. □

Corollary 8.3. *The Bézier curve β_1 is ambient isotopic to its control polygon $K_{1,4}$, the trefoil.*

Theorem 8.4. *The ambient isotopy between K_0 and K_1 generates a Bézier curve with a self-intersection.*

Proof. The perturbation of the control point $(-10, 60, 58)$ to $(10, 60, 58)$ creates a homotopy on the Bézier curve β_0 to β_1, defined over the interval $[0,1]$. If for all values of $t \in [0,1]$, the perturbed Bézier curve was simple, then the homotopy would be an isotopy between β_0 and β_1. However, since β_0 and β_1 have differing prime knot types, this cannot be. So, for some value $\tilde{t} \in [0,1]$, the corresponding Bézier curve must have a self-intersection. □

9. Conclusion and Future Work

An example is shown of a closed Bézier curve and its control polygon which are both the unknot. A perturbation of one vertex is shown to cause the perturbed Bézier curve to be the trefoil, while its control polygon remains the unknot. This transition demonstrates that there must have been an intermediate state where a self-intersection occurred in the transforming Bézier curves. These topological differences between the mathematical representation and its PL approximation are of interest in computer graphics and animation. Visual evidence previously existed, but the only supportive mathematics relied on floating point arithmetic which left open the question of whether an intermediate intersection could be rigorously proven. The formal proof presented relies on the implementation of exact, integer computations to resolve that open question.

Comparisons between the exact techniques and certifiable numeric methods merit further consideration, as it may often be of interest to specify a neighborhood in which a self-intersection is known to exist. The present example was quite carefully constructed to show the self-intersection and robust numerical methods are likely to have broader scope for applications.

Acknowledgements. *The authors acknowledge, with appreciation, the contributions of*

- *D. Marsh, for software that generated experimental visualizations and related computations,*
- *the reviewers, for singularly comprehensive and constructive comments, and*
- *the editors, for their keen insight and informed perspective in selecting those reviewers.*

References

[1] Cybergloves. http://www.cyberglovesystems.com/cyberglove-iii/.
[2] ManusVR. https://manus-vr.com/.
[3] Virtual motion labs. http://www.virtualmotionlabs.com/.
[4] N. Amenta, T. J. Peters and A. C. Russell, Computational topology: Ambient isotopic approximation of 2-manifolds, Theoretical Computer Science 305 (2003), 3–15.
[5] L. E. Andersson, S. M. Dorney, T. J. Peters and N. F. Stewart, Polyhedral perturbations that preserve topological form, CAGD 12, no. 8 (1995), 785–799.
[6] L. E. Andersson, T. J. Peters and N. F. Stewart, Selfintersection of composite curves and surfaces, CAGD 15 (1998), 507–527.
[7] M. A. Armstrong, Basic Topology, Springer, New York, 1983.
[8] R. H. Bing, The Geometric Topology of 3-Manifolds, American Mathematical Society, Providence, RI, 1983.
[9] J. Bisceglio, T. J. Peters, J. A. Roulier and C. H. Sequin, Unknots with highly knotted control polygons, CAGD 28, no. 3 (2011), 212–214.

© AGT, UPV, 2019

[10] F. Chazal and D. Cohen-Steiner, A condition for isotopic approximation, Graphical Models 67, no. 5 (2005), 390–404.
[11] T. Culver, J. Keyser and D. Manocha, Exact computation of the medial axis of a polyhedron, Computer Aided Geometric Design 21, no. 1 (2004), 65–98.
[12] T. Etiene, L. G. Nonato, C. E. Scheidegger, J. Tierny, T. J. Peters, V. Pascucci, R. M. Kirby and C. T. Silva, Topology verification for isosurface extraction, IEEE Trans. Vis. Comput. Graph. 18, no. 6 (2012), 952–965.
[13] G. E. Farin, Curves and Surfaces for Computer-Aided Geometric Design: A Practical Guide, Academic Press, Inc., 1996.
[14] J. D. Foley, A. van Dam, S. K. Feiner and J. F. Hughes, Computer Graphics: Principles and Practice (2Nd Ed.), Addison-Wesley Longman Publishing Co., Inc., Boston, MA, USA, 1990.
[15] D. Jiang and N. F. Stewart, Backward error analysis in computational geometry, Springer Berlin Heidelberg, Berlin, Heidelberg, 2006, pp. 50–59.
[16] K. E. Jordan, J. Li, T. J. Peters and J. A. Roulier, Isotopic equivalence from Bézier curve subdivision for application to high performance computing, CAGD 31 (2014), 642–655.
[17] K. E. Jordan, L. E. Miller, E. L. F. Moore, T. J. Peters and A. Russell, Modeling time and topology for animation and visualization with examples on parametric geometry, Theoretical Computer Science 405 (2008), 41–49.
[18] L. Kettner, K. Mehlhorn, S. Pion, S. Schirra and C. Yap, Classroom examples of robustness problems in geometric computations, Computational Geometry 40, no. 1 (2008), 61–78.
[19] R. M. Kirby and C. T. Silva, The need for verifiable visualization, IEEE Computer Graphics and Applications September/October (2008), 1–9.
[20] J. M. Lane and R. F. Riesenfeld, A theoretical development for the computer generation and display of piecewise polynomial surfaces, IEEE, PAMI-2 no. 1, January 1980.
[21] J. Li and T. J. Peters, Isotopic convergence theorem, Journal of Knot Theory and Its Ramifications 22, no. 3 (2013).
[22] J. Li, T. J. Peters, D. Marsh and K. E. Jordan, Computational topology counterexamples with 3D visualization of Bézier curves, Applied General Topology 13, no. 2 (2012), 115–134.
[23] G. McGill, Molecular movies coming to a lecture near you, Cell 133, no. 7 (2008), 1127–1132.
[24] J. Munkres, Topology, Prentice Hall, 2nd edition, 1999.
[25] M. Neagu, E. Calcoen and B. Lacolle, Bézier curves: topological convergence of the control polygon, 6th Int. Conf. on Mathematical Methods for Curves and Surfaces, Vanderbilt (2000), pp. 347–354.
[26] J. Peters and X. Wu, On the optimality of piecewise linear max-norm enclosures based on SLEFES, International Conference on Curves and Surfaces, Saint-Malo, France, 2002.
[27] L. Piegl and W. Tiller, The NURBS Book, Springer, New York, 1997.
[28] C. H. Sequin, Spline knots and their control polygons with differing knottedness, http://www.eecs.berkeley.edu/Pubs/TechRpts/2009/EECS-2009-152.html.
[29] M. Wertheim and K. Millett, Where the wild things are: An interview with Ken Millett, Cabinet 20, 2006.

© AGT, UPV, 2019

Appendix A. Subdivision Data

The following two tables list the vertices for both the original and perturbed control polygons, each after 4 subdivisions. The strict monotonicity of specific coordinates is indicated for each subdivided control polygon.

In Table I for subdivision of K_0, the sixteen control polygons are denoted by P[0], ..., P[15] and all consecutive control polygons are separated by half-planes. Between P[0] and P[1] the separating plane is the XZ plane at the y-value of the last point of P[0]. Between P[1] and P[2] the separating plane is the XZ plane at the y-value of the last point of P[1]. For all others, it is a YZ plane at the x value of the shared subdivision point.

In Table II for subdivision of K_1, the sixteen control polygons are denoted by Q[0], ..., Q[15] and all consecutive control polygons are separated by half-planes. Between Q[9] and Q[10] the separating plane is the XZ plane at the y-value of the last point of P[0]. Between Q[14] and Q[15] the separating plane is the XZ plane at the y-value of the last point of P[14]. For all others, it is a YZ plane at the x value of the shared subdivision point.

A notational change for points occurs in Appendix A. In the preceding narrative, points are denoted by parentheses in the format of (x, y, z). Within Appendix A, points are bounded by the set brackets in the format of $\{x, y, z\}$, as the required syntax within Mathematica, where many of the computations were performed. For integrity of the data, it was judged best to report the points using this alternative formatting.

The code used and its output is posted for public access at

`https://github.com/kmarinelli/AGT_2018_TP_KM`

Table I: Subdivision Points from 4 Iterations on K_0

```
P[0]: Y,Z                                  {  319961600, -12190760448,-7488402432},
{          0, 4831838208,10737418240 },    {  553614080, -11913360640,-7687345664},
{ -503316480, 1342177280,8388608000 },     {  774794880, -11567678336,-7779114240},
{ -859832320, -1562378240,6249512960 },    {  977745600, -11173260096,-7774340480}
{ -1092485120, -3959685120,4313317376 },
{ -1221918720, -5918269440,2572288000 }, P[3]; X,Y,Z
{ -1266603520, -7498398720,1017953280 },   {  977745600, -11173260096,-7774340480},
{ -1242964800, -8753032512,-358732160 }    { 1180696320, -10778841856,-7769566720 },
                                           { 1365416960, -10335687680,-7668250624 },
P[1]:  X,Y,Z                               { 1526149120, -9863344128,-7481024512 },
{ -1242964800, -8753032512,-358732160},    { 1658634240, -9377366016,-7218495488 },
{ -1219326080, -10007666304,-1735417600}, { 1759969280, -8890023936,-6891110400 },
{ -1127363840, -10936804608,-2934453760}, { 1828454400, -8410890240,-6509035520 }
{ -983503360, -11593406976,-3964886016},
{ -802124800, -12023124992,-4836333568}, P[4]: Y,Z
{ -595691520, -12265252864,-5558824960}, { 1828454400, -8410890240,-6509035520 },
{ -374886400, -12353556480,-6142648320}    { 1896939520, -7931756544,-6126960640 },
                                           { 1932574720, -7460831232,-5690195968 },
P[2]: X                                    { 1933660160, -7007686656,-5208907776 },
{ -374886400, -12353556480,-6142648320}, { 1899699200, -6579196928,-4692981760 },
{ -154081280, -12441860096,-6726471680}, { 1831246080, -6180123904,-4151902720 },
{   81095680, -12376339456,-7171627008}, { 1729745600, -5813581632,-3594648960 }
```

```
                                        { -4792325120, -6640727040,2465638400 },
P[5]: X,Y,Z                             { -4681285120, -6883653120,2016869376 },
{ 1729745600, -5813581632,-3594648960 }, { -4523326720, -7126519040,1534876160 },
{ 1628245120, -5447039360,-3037395200 }, { -4318696320, -7367136640,1026778880 },
{ 1493697280, -5113027840,-2463966720 }, { -4068961600, -7602868032, 500941440 }
{ 1327546880, -4814661120,-1883341824 },
{ 1132129280, -4553405440,-1303992320 }, P[11]: X,Y,Z
{  910510080, -4329543680,-733777920 },  { -4068961600, -7602868032, 500941440},
{  666316800, -4142518272,-179855360 }   { -3819226880, -7838599424, -24896000},
                                        { -3524387840, -8069444608,-568473600},
P[6]: X,Y,Z                             { -3186012160, -8292765696,-1121427456},
{  666316800, -4142518272,-179855360 },  { -2806988800, -8505475072,-1674149888},
{  422123520, -3955492864, 374067200 },  { -2391736320, -8703770624,-2215772160},
{  155356160, -3805303808, 911697920 },  { -1946419200, -8882749440,-2734161920}
{ -130357760, -3691393536,1425880064 },
{ -430828800, -3612364032,1910159872 },  P[12]: X,Y,Z
{ -741473920, -3566319744,2358877440 },  { -1946419200, -8882749440,-2734161920},
{ -1057492800, -3551088960,2767242880 }  { -1501102080, -9061728256,-3252551680 },
                                        { -1025720320, -9221390336,-3747708928 },
P[7]: X,Z                               { -526438400, -9356832768,-4207501312 },
{ -1057492800, -3551088960,2767242880 }, {  -11166720, -9462051840,-4618532864 },
{ -1373511680, -3535858176,3175608320 }, {  510222080, -9529556736,-4966141440 },
{ -1694904320, -3551440896,3543621632 }, { 1025668800, -9549861696,-5234410880 }
{ -2016870400, -3595665408,3866492928 },
{ -2334392320, -3666083840,4140302336 }, P[13]: X
{ -2642411520, -3760193536,4362076160 }, { 1025668800, -9549861696,-5234410880 },
{ -2936012800, -3875536896,4529848320 }  { 1541115520, -9570166656,-5502680320 },
                                        { 2050620160, -9543271680,-5691610624 },
P[8]: X,Y                               { 2542123520, -9459691008,-5785285632 },
{ -2936012800, -3875536896,4529848320 }, { 3001379840, -9307943936,-5766535168 },
{ -3229614080, -3990880256,4697620480 }, { 3411732480, -9074046976,-5616947200 },
{ -3508797440, -4127457280,4811390976 }, { 3753881600, -8740884480,-5316894720 }
{ -3768647680, -4282810368,4869193728 },
{ -4004392960, -4454526976,4870070272 }, P[14]: Y,Z
{ -4211589120, -4640339456,4814131200 }, { 3753881600, -8740884480,-5316894720 },
{ -4386312000, -4838103360,4702602880 }  { 4096030720, -8407721984,-5016842240 },
                                        { 4369976320, -7975293952,-4566325248 },
                                        { 4556418560, -7426484736,-3945716736 },
P[9]: Y,Z                               { 4633414400, -6741046528,-3134174720 },
{ -4386312000, -4838103360,4702602880 }, { 4576145280, -5894969984,-2109669120 },
{ -4561034880, -5035867264,4591074560 }, { 4356676800, -4859733312,-849023360 }
{ -4703284480, -5245582592,4423956992 },
{ -4809136640, -5465104896,4202476544 }, P[15]: X,Y,Z
{ -4875187200, -5692412928,3928975360 }, { 4356676800, -4859733312,-849023360 },
{ -4898744320, -5925586944,3606958080 }, { 4137208320, -3824496640, 411622400 },
{ -4878028800, -6162665472,3241123840 }  { 3755540480, -2600099840,1908408320 },
                                        { 3183738880, -1158021120,3664510976 },
P[10]: X,Y,Z                            { 2390753280,  534773760,5704253440 },
{ -4878028800, -6162665472,3241123840 }, { 1342177280, 2516582400,8053063680 },
{ -4857313280, -6399744000,2875289600 }, {          0, 4831838208,10737418240 }
```

Table II: Subdivision Points from 4 Iterations on K_1

```
Q[0]: Y,Z
{         0, 4831838208,10737418240 },
{ -503316480, 1342177280,8388608000 },
{ -859832320, -1562378240,6249512960 },
{ -1089863680, -3959685120,4312924160 },
{ -1212088320, -5918269440,2570813440 },
{ -1243563520, -7498398720,1014497280 },
{ -1199764800, -8753032512,-365212160 }

Q[1]: X, Y, Z
{ -1199764800, -8753032512,-365212160 },
{-1155966080, -10007666304,-1744921600},
{ -1036893440, -10936804608,-2948024320 },
{ -858022400, -11593406976,-3983708160 },
{ -633246720, -12023124992,-4861665280 },
{ -374917120, -12265252864,-5591941120 },
{  -93900800, -12353556480,-6184796160 }

Q[2]: X
{  -93900800, -12353556480,-6184796160 },
{  187115520, -12441860096,-6777651200 },
{  490818560, -12376339456,-7233085440 },
{  806341120, -12190760448,-7561359360 },
{ 1124299520, -11913360640,-7772948480 },
{ 1436734080, -11567678336,-7878405120 },
{ 1737028800, -11173260096,-7888232960 }

Q[3]: X, Y, Z
{ 1737028800, -11173260096,-7888232960 },
{ 2037323520, -10778841856,-7898060800 },
{ 2325478400, -10335687680,-7812259840 },
{ 2594877440, -9863344128,-7641333760 },
{ 2840248320, -9377366016,-7395737600 },
{ 3057582080, -8890023936,-7085752320 },
{ 3244032000, -8410890240,-6721372160 }

Q[4]: X, Y, Z
{ 3244032000, -8410890240,-6721372160 },
{ 3430481920, -7931756544,-6356992000 },
{ 3586048000, -7460831232,-5938216960 },
{ 3707883520, -7007686656,-5475041280 },
{ 3794304000, -6579196928,-4977172480 },
{ 3844686080, -6180123904,-4453918720 },
{ 3859345600, -5813581632,-3914088960 }

Q[5]: Y, Z
{ 3859345600, -5813581632,-3914088960 },
{ 3874005120, -5447039360,-3374259200 },
{ 3852942080, -5113027840,-2817853440 },
{ 3796472320, -4814661120,-2253680640 },
{ 3705850880, -4553405440,-1690050560 },
{ 3583150080, -4329543680,-1134673920 },
{ 3431116800, -4142518272,-594575360 }

Q[6]: X, Y, Z
{ 3431116800, -4142518272,-594575360 },
{ 3279083520, -3955492864, -54476800 },
{ 3097717760, -3805303808, 470343680 },
{ 2889766400, -3691393536, 972861440 },
{ 2658650880, -3612364032,1446737920 },
{ 2408324480, -3566319744,1886407680 },
{ 2143108800, -3551088960,2287152640 }

Q[7]: X, Z
{ 2143108800, -3551088960,2287152640 },
{ 1877893120, -3535858176,2687897600 },
{ 1597788160, -3551440896,3049717760 },
{ 1307115520, -3595665408,3367895040 },
{ 1010565120, -3666083840,3638558720 },
{  713031680, -3760193536,3858759680 },
{  419430400, -3875536896,4026531840 }

Q[8]: X, Y
{  419430400, -3875536896,4026531840 },
{  125829120, -3990080256,4194304000 },
{ -163840000, -4127457280,4309647360 },
{ -444661760, -4282810368,4370595840 },
{ -711700480, -4454526976,4376166400 },
{ -960184320, -4640339456,4326420480 },
{ -1185710400, -4838103360,4222512640 }

Q[9]: X, Y, Z
{ -1185710400, -4838103360,4222512640 },
{ -1411236480, -5035867264,4118604800 },
{ -1613804800, -5245582592,3960535040 },
{ -1789012480, -5465104896,3749457920 },
{ -1932825600, -5692412928,3487621120 },
{ -2041784320, -5925586944,3178414080 },
{ -2113228800, -6162665472,2826403840 }

Q[10]: Y, Z
{ -2113228800, -6162665472,2826403840 },
{ -2184673280, -6399744000,2474393600 },
{ -2218603520, -6640727040,2079580160 },
{ -2212359680, -6883653120,1646530560 },
{ -2164081920, -7126519040,1180989440 },
{ -2072936320, -7367136640, 689914880 },
{ -1939361600, -7602868032, 181501440 }

Q[11]: X, Y, Z
{ -1939361600, -7602868032, 181501440 },
{ -1805786880, -7838599424,-326912000 },
```

```
{ -1629783040, -8069444608,-852664320 }, { 3752929280, -9074046976,-5668126720 },
{ -1411788800, -8292765696,-1387560960 },{ 4034867200, -8740884480,-5359042560 }
{ -1153515520, -8505475072,-1922170880 },
{ -858193920, -8703770624,-2445803520 }, Q[14]: Y, Z
{ -530841600, -8882749440,-2946498560 }  { 4034867200, -8740884480,-5359042560 },
                                         { 4316805120, -8407721984,-5049958400 },
Q[12]: X, Y, Z                           { 4538854400, -7975293952,-4591656960 },
{ -530841600, -8882749440,-2946498560 }, { 4681899520, -7426484736,-3964538880 },
{ -203489280, -9061728256,-3447193600 }, { 4723884800, -6741046528,-3147745280 },
{  155893760, -9221390336,-3924951040 }, { 4639505280, -5894969984,-2119173120 },
{  542289920, -9356832768,-4367810560 }, { 4399876800, -4859733312,-855503360 }
{  948894720, -9462051840,-4762542080 },
{ 1366849280, -9529556736,-5094635520 }, Q[15]: X, Y, Z
{ 1784952000, -9549861696,-5348303360 }  { 4399876800, -4859733312,-855503360 },
                                         { 4160248320, -3824496640, 408166400 },
Q[13]: X                                 { 3765370880, -2600099840,1906933760 },
{ 1784952000, -9549861696,-5348303360 }, { 3186360320, -1158021120,3664117760 },
{ 2203054720, -9570166656,-5601971200 }, { 2390753280,  534773760,5704253440 },
{ 2621305600, -9543271680,-5777213440 }, { 1342177280, 2516582400,8053063680 },
{ 3028503040, -9459691008,-5858242560 }, {          0, 4831838208,10737418240 }
{ 3411102720, -9307943936,-5827993600 },
```